

Digital color cameras - 2 - Spectral response

Poorvi L. Vora, Joyce E. Farrell,
Hewlett-Packard Laboratories, 1501 Page Mill Road, Palo Alto, CA 94304
Phone: (415) 857-2457, Fax: (415) 857-4691
Email: { poorvi, farrell }@ hpl.hp.com
Jerome D. Tietz, David H. Brainard
Dept. of Psychology, University of California at Santa Barbara
Santa Barbara, CA 93106
Phone: (805) 893-2011, Fax: (805) 893-4303
Email: {tietz, brainard }@ psych.ucsb.edu

Abstract

This report describes the spectral calibration of two digital color cameras, the Kodak DCS-200 and the Kodak DCS-420. We used previous work to model the output of the cameras in terms of the spectral sensitivities of the color sensors. We took measurements of the camera output for narrow-band spatially uniform scenes and used this data to estimate the sensor spectral sensitivities. The estimated spectral sensitivities were used to generate predicted RGB values which were compared to the measurements. The error between the predicted and measured values is a measure of the accuracy of the sensitivity estimates. For our estimates, this error is comparable to our estimates of the camera response variability. We also used the sensor estimates to predict the response of the DCS-200 to an independently acquired image. This prediction error was also small.

1 Introduction

To process data from digital color cameras, it is often necessary to know the spectral response properties of the camera’s sensors. For example, many demosaicing [1], color correction [13] and illuminant estimation algorithms [4, 5] require this knowledge. In addition, the intrinsic color quality of an image depends on the spectral characteristics of the sensors [2, 7, 12, 14, 15] used. Thus an important component of characterizing a digital color camera is measuring its sensor spectral response functions.

We describe calibration of the spectral response of two color cameras, a Kodak DCS-200 and a Kodak DCS-420. The calibration procedure is based on the response models we developed previously for these cameras [10]. We use the resulting estimates in work where we simulate camera responses [9, 11].

The report is organized as follows. Section 2 describes the calibration data we collected. Sections 3 and 4 describe two different procedures for estimating the camera sensor spectral response functions. These are the *simple estimation* procedure and the *Wiener estimation* procedure respectively. Section 5 examines how well our estimates of the DCS-200 can predict the camera responses for images of the Macbeth ColorChecker Chart (MCC). Section 6 presents conclusions.

2 Methods

In a companion report [10], we showed that the following equation relates the output of a camera sensor r to the spectral response of the sensor $s(\lambda)$, the incident radiant power $i(\lambda)d\lambda$, the exposure time e and the measurement noise n :

$$r = \mathcal{F}(e \int_{\lambda_l}^{\lambda_h} s(\lambda)i(\lambda)d\lambda + n) \tag{1}$$

The wavelengths λ_l and λ_h are the limits beyond which the spectral response of the sensor is zero. The function \mathcal{F} is a static non-linearity. We determined this function empirically for the DCS-420. For the DCS-200, the function is simply the identity.

We measured the spectral response functions for two color CCD cameras, the Kodak DCS-200 and Kodak DCS-420. For both cameras, we used the 8-bit acquisition software provided by Kodak. In this mode, the response of the DCS-200 is linear with intensity while the response of the DCS-420 is non-linear [10]. The camera apertures were kept fixed through all the experiments reported here, at f4 for the DCS-420 and f5.6 for the DCS-200. These are the same aperture settings we used to determine the camera response models.

To calibrate the camera spectral sensitivities, we measured camera responses to narrow band illumination. We created narrow band stimuli using light from a tungsten source passed through a monochromator (Bausch and Lomb, 1350 grooves/mm) and imaged onto a white reflectance standard (PhotoResearch RS-2). We measured the integrated radiance of each narrow band stimulus using a spectroradiometer (PhotoResearch PR-650). The camera and the radiometer were placed at similar geometric positions with respect to the reflectance standard.

It is difficult to measure the exact spectral power distributions of narrow band sources using the PR-650, since the instrument itself has a bandwidth of 8nm, comparable to that of the narrow band lights. When we performed calculations that required an estimate of the spectral power distributions, we modeled them as gaussians with a standard deviation of 7.5 nm and scaled so that they had the same integrated radiance as our measurements.

We extracted red, green, and blue (R, G, and B) sensor responses from the camera images and averaged these over a rectangular section in the center of the image (64×64 pixels for the DCS-420 and 30×25 pixels for the DCS-200).

For the DCS-200, we excluded measurements outside of the camera's linear operating range

- i.e. response values below 20 or above 240. We corrected the measured responses for the camera dark current by subtracting our estimate of its mean value (13.6 response units). For the DCS-420, we used the method described in the companion report [10] to obtain linearized response values.

To extend the dynamic range of the cameras, we varied the exposure duration across measurements. We normalized response data across exposure setting by dividing the measured response by the response duration. Thus the units of our calibrations are response per second of exposure. Where we had multiple measurements for the same incident illuminant, we used the data corresponding to the maximum non-saturated response. Tables 7 - 9 and Tables 10 - 12 in the appendix provide the response data we used for each camera.

3 Simple Estimates

To perform calculations, we write a sampled version of equation (1) that describes the entire calibration data set. Let \mathbf{r} , \mathbf{g} , and \mathbf{b} be vectors representing the R, G, B readings to a series of narrowband lights. The vectors \mathbf{r} , \mathbf{g} , and \mathbf{b} have K_r , K_g and K_b entries respectively, one for each of the narrowband stimuli used to calibrate the corresponding sensor. Let the full spectrum of the i^{th} narrowband light be $s_i(\lambda)$, and let the unknown camera spectral sensitivities be $c_r(\lambda)$, $c_g(\lambda)$ and $c_b(\lambda)$. From equation (1) we have,

$$\mathbf{r} = \mathcal{F} \left(\begin{bmatrix} e(1) \sum_j c_r(\lambda_l + j\Delta\lambda) s_1(\lambda_l + j\Delta\lambda) \Delta\lambda \\ \vdots \\ e(i) \sum_j c_r(\lambda_l + j\Delta\lambda) s_i(\lambda_l + j\Delta\lambda) \Delta\lambda \\ \vdots \\ e(K_r) \sum_j c_r(\lambda_l + j\Delta\lambda) s_{K_r}(\lambda_l + j\Delta\lambda) \Delta\lambda \end{bmatrix} + \mathbf{n} \right) \quad (2)$$

where \mathbf{n} is a vector representing measurement noise with variation about the average dark noise value, $\Delta\lambda$ is the wavelength sampling for the radiometric measurements, and $e(i)$ is the exposure setting for the i^{th} measurement. The function \mathcal{F} is applied pointwise to each component of the vector it acts on. It is the identity for the DCS-200 and the calibrated

static non-linearity for the DCS-420. Equations similar to the one above can be written for the readings \mathbf{g} and \mathbf{b} .

The equations for $c_r(\lambda)$, $c_g(\lambda)$ and $c_b(\lambda)$ may be solved in a number of different ways. In the rest of this section and in the following section we discuss two possibilities.

The illumination incident on the camera is narrow-band. This fact may be used to approximate equation (2) by

$$\mathbf{r} = \mathcal{F} \left(\begin{bmatrix} e(1)c_r(\lambda_1) \sum_j s_1(\lambda_l + j\Delta\lambda)\Delta\lambda \\ \vdots \\ e(i)c_r(\lambda_i) \sum_j s_i(\lambda_l + j\Delta\lambda)\Delta\lambda \\ \vdots \\ e(K_r)c_r(\lambda_{K_r}) \sum_j s_{K_r}(\lambda_l + j\Delta\lambda)\Delta\lambda \end{bmatrix} + \mathbf{n} \right)$$

where λ_i is the wavelength of the peak of the i^{th} incident illumination. By ignoring the noise variability, we estimate the sensor response function $c_r(\lambda_i)$ as

$$c_r(\lambda_i) = \frac{\mathcal{F}^{-1}(r_i) - \bar{n}}{e(i) \sum_j s_i(\lambda_l + j\Delta\lambda)\Delta\lambda} \quad (3)$$

where r_i is the i^{th} component of \mathbf{r} , the quantity $\sum_j s_i(\lambda_l + j\Delta\lambda)\Delta\lambda$ is the integrated radiance of the i^{th} narrowband stimulus and \bar{n} is the mean of the noise. For CCD cameras, this mean is typically non-zero.

Equation (3) is the ‘simple’ estimate of Hubel et al [3]. The function \mathcal{F} is the identity for the DCS-200 and $\bar{n} = 13.6$ from the experiments detailed in [10]. For the DCS-420, the quantity $\mathcal{F}^{-1}(\mathbf{r}_i) - \bar{n}$ may be obtained from the calibration curve provided in [10].

Figure 1 shows plots of the simple estimates obtained for the DCS-200 and Figure 2 those for the DCS-420. The plotted estimates are interpolated from the raw estimates to a 5 nm wavelength spacing in the range 380 nm to 780 nm. In the interpolation procedure, values for wavelengths outside the range where we had data were set to zero. Tables 13 and 14 provided in the appendix tabulate the estimated sensor responses.

The expression

$$\mathcal{F}(e(i) \sum c_r(\lambda_j) s_i(\lambda_j) \Delta \lambda_j + \bar{n}) \quad (4)$$

was used to calculate RGB values for sensors with the estimated spectral sensitivities. The function \mathcal{F} was taken to be the identity for the DCS-200. For the DCS-420, an inverse curve based on the previous calibration was used. We compared the predicted RGB values to the measurements. Figure 3 shows plots of the measured R, G and B values against the values indicated by expression (4) for the DCS-200, while Figure 4 shows the same for the DCS-420. Table 1 shows the statistics of the estimation error for the DCS-200 and Table 2 for the DCS-420. In these tables absolute error denotes the absolute value of the difference between measured and predicted values. The standard deviation of the camera dark noise is listed for comparison with the rms error associated with the sensor estimates.

Table 1: Statistics of Estimation Error - DCS-200 - Simple Estimate. RMS value of variation from linearity of DCS-200 is 1.45 [10].

| Sensor Type | Mean of Absolute Error | Mean of Absolute % Error | RMS Error | Camera Noise Std. Deviation | Maximum Absolute Error | Maximum Absolute % Error |
|-------------|------------------------|--------------------------|-----------|-----------------------------|------------------------|--------------------------|
| Red | 1.34 | 1.60 | 3.68 | 0.88 | 16.46 | 20.27 |
| Green | 0.53 | 1.10 | 0.99 | 0.89 | 4.09 | 1.09 |
| Blue | 0.50 | 1.29 | 0.89 | 0.90 | 3.48 | 9.50 |

Table 2: Statistics of Estimation Error - DCS-420 - Simple Estimate. RMS value of variation from modelling curve of DCS-420 is 0.50 [10].

| Sensor Type | Mean of Absolute Error | Mean of Absolute % Error | RMS Error | Camera Noise Std. Deviation | Maximum Absolute Error | Maximum Absolute % Error |
|-------------|------------------------|--------------------------|-----------|-----------------------------|------------------------|--------------------------|
| Red | 0.83 | 0.88 | 1.59 | 0.49 | 7.47 | 6.00 |
| Green | 0.57 | 0.88 | 0.74 | 0.47 | 1.96 | 4.17 |
| Blue | 0.59 | 0.91 | 0.78 | 0.47 | 2.36 | 3.99 |

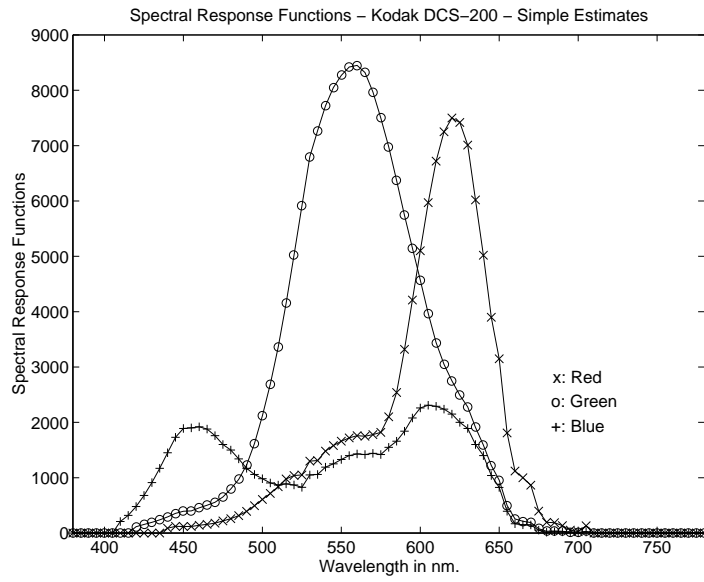


Figure 1: Spectral Response Functions of the Kodak DCS-200 - Simple Estimate.

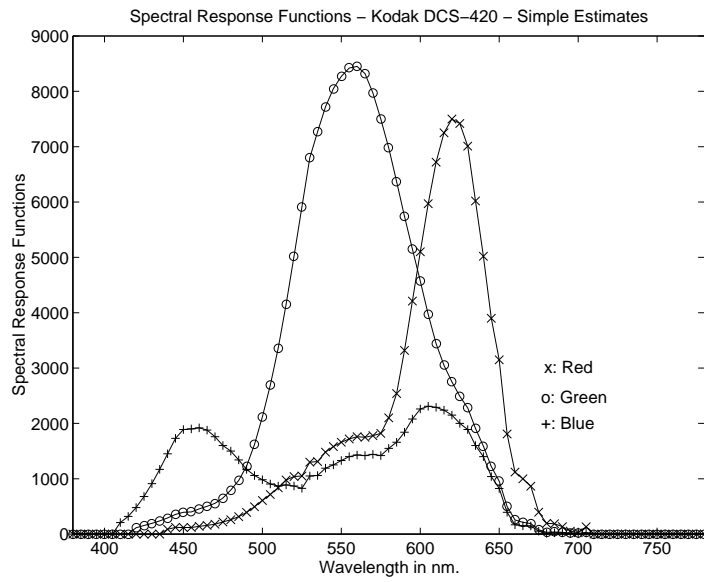


Figure 2: Spectral Response Functions of the Kodak DCS-420 - Simple Estimate.

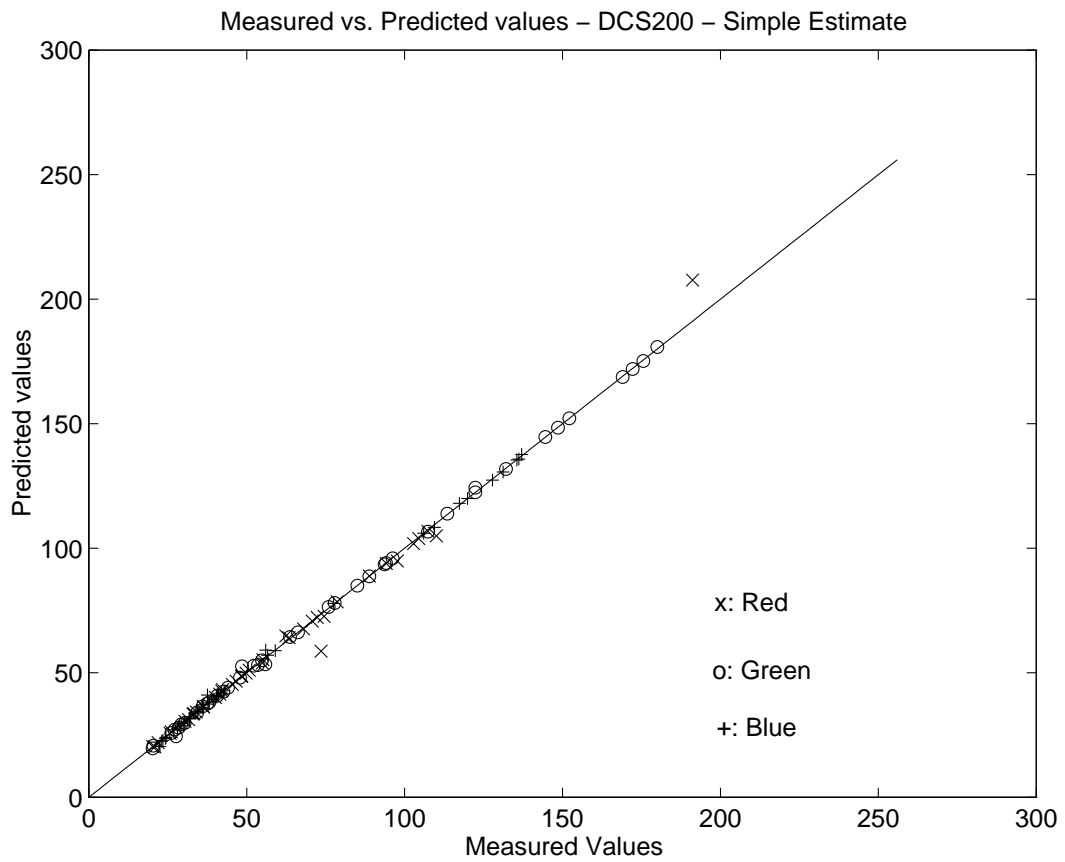


Figure 3: Measured vs. Predicted Values Kodak DCS-200 - Simple Estimate.

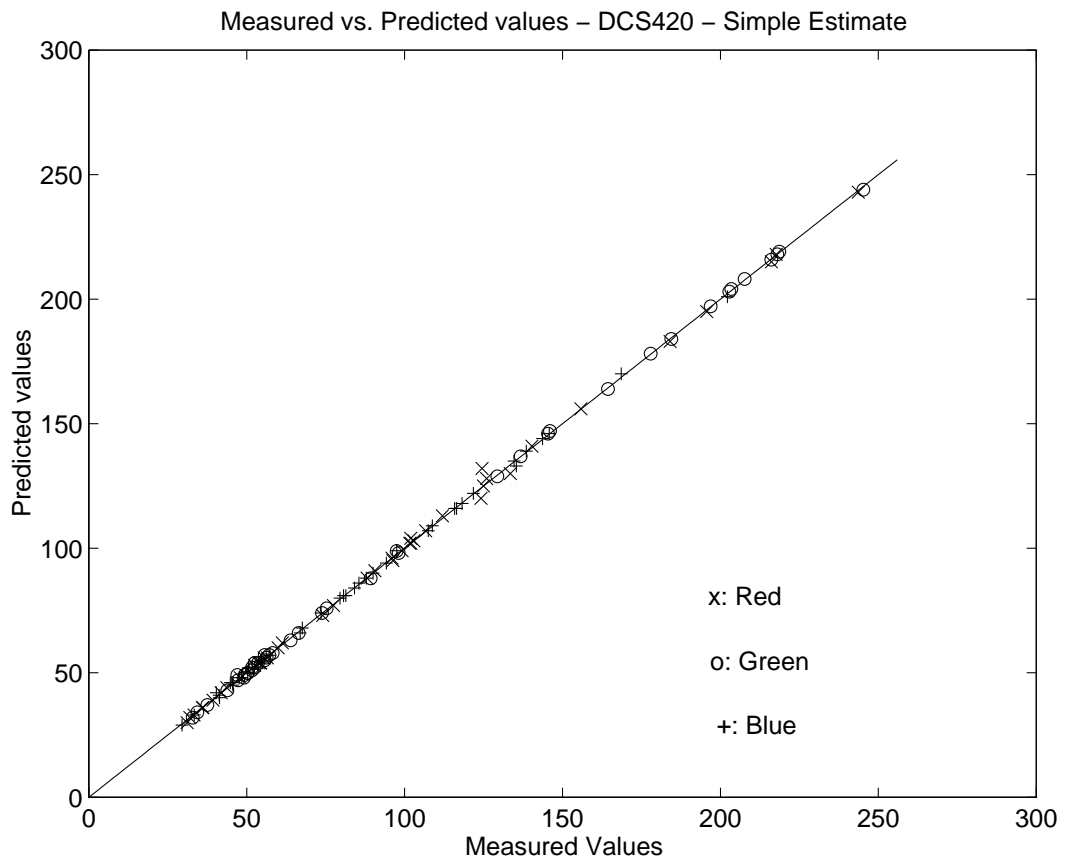


Figure 4: Measured vs. Predicted Values Kodak DCS-420 - Simple Estimate.

4 Wiener Estimates

The simple estimation procedure neglects the variability in the sensor responses. It also neglects the fact that the width of the spectral power distribution of the narrowband light source is non-zero. Error in the response measurement for a narrowband light at one wavelength directly affects the sensitivity estimate for that wavelength, as does error in the measure of the power of the incident light. It is possible to employ more sophisticated estimation techniques that take camera response variability (noise variation) and the non-zero width of the spectral power distribution of incident light into account when producing the estimates. In this section, we describe how we used Wiener estimation to obtain a second set of sensor estimates.

We begin by rewriting the equation to be solved (equation 2) in matrix form. Let \mathbf{y} represent the linearized and normalized sensor measurements for a particular sensor. That is, let the i^{th} entry of \mathbf{y} be $\mathbf{y}_i = \frac{\mathcal{F}^{-1}(r_i) - \bar{n}}{e(i)}$. Let \mathbf{x} be a vector representing the sensor estimate to be obtained represented at discrete sample wavelengths. We can write $\mathbf{y} = \mathbf{H}\mathbf{x} + \mathbf{n}_0$ where \mathbf{H} is a matrix whose i^{th} row is the sampled spectrum of the i^{th} narrowband stimulus and \mathbf{n}_0 is a vector representing zero-mean additive noise. Our goal is to solve this system of linear equations for \mathbf{x} . This is a standard problem. Pratt [6] provides the Wiener estimate for problems of this form. We used a variant of this procedure that is guaranteed to produce all positive estimates.

The Wiener procedure requires that we regard the quantity to be estimated (\mathbf{x}) as a gaussian random variable with known mean and covariance. We took the mean $\bar{\mathbf{x}}$ to be the simple estimate obtained in the previous section and constructed the covariance matrix $\kappa_{\mathbf{x}}$ by assuming that \mathbf{x} was the result of a first-order discrete Gauss-Markov process whose variance was equal to the variance of the entries of $\bar{\mathbf{x}}$ and whose entry-to-entry correlation was equal to the correlation between neighboring entries of $\bar{\mathbf{x}}$. We assumed that the entries of \mathbf{n}_0 were

independently and identically distributed with mean zero and variance equal to 2% of the maximum linearized sensor response (after correction for non-linearity, mean noise level, and exposure duration). We did this for each sensor.

The DCS-200 estimates are plotted in Figure 5, the predicted RGB values in Figure 7 and the error statistics are listed in Table 3. The DCS-420 estimates are plotted in Figure 6, the predicted RGB values in Figure 8 and the error statistics listed in Table 4. The plotted estimates are interpolated from the raw estimates to a 5 nm wavelength spacing in the range 380 nm to 780 nm. In the interpolation procedure, values for wavelengths outside the range where we had data were set to zero. Tables 15 and 16 provided in the appendix tabulate the estimated sensor responses.

Table 3: Statistics of Estimation Error - DCS-200 - Wiener Estimates. RMS value of variation from linearity of DCS-200 is 1.45 [10].

| Sensor Type | Mean of Absolute Error | Mean of Absolute % Error | RMS Error | Noise Std. Deviation | Maximum Absolute Error | Maximum Absolute % Error |
|-------------|------------------------|--------------------------|-----------|----------------------|------------------------|--------------------------|
| Red | 0.53 | 0.65 | 1.42 | 0.88 | 8.07 | 4.22 |
| Green | 0.57 | 0.55 | 0.46 | 0.89 | 1.34 | 2.65 |
| Blue | 0.28 | 0.62 | 0.41 | 0.90 | 1.58 | 4.20 |

Table 4: Statistics of Estimation Error - DCS-420 - Wiener Estimates. RMS value of variation from modelling curve of DCS-420 is 0.50 [10].

| Sensor Type | Mean of Absolute Error | Mean of Absolute % Error | RMS Error | Noise Std. Deviation | Maximum Absolute Error | Maximum Absolute % Error |
|-------------|------------------------|--------------------------|-----------|----------------------|------------------------|--------------------------|
| Red | 0.40 | 0.51 | 0.62 | 0.49 | 2.47 | 3.69 |
| Green | 0.35 | 0.55 | 0.46 | 0.47 | 1.34 | 2.65 |
| Blue | 0.47 | 0.66 | 0.59 | 0.47 | 1.50 | 2.63 |

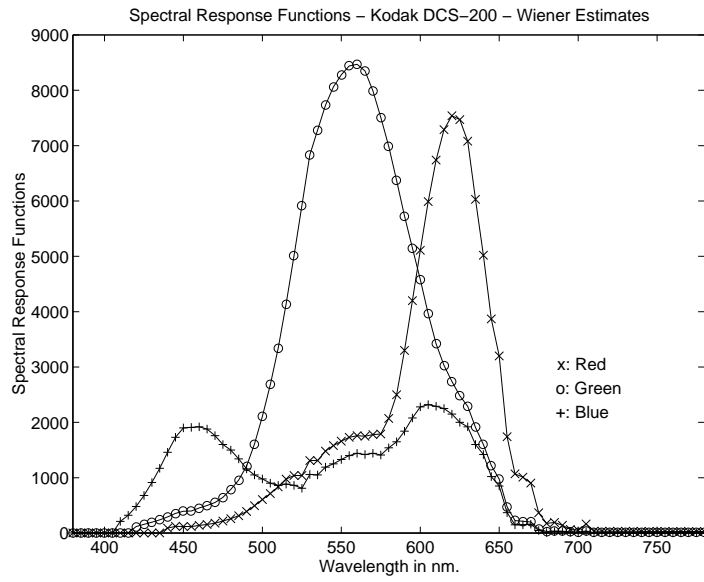


Figure 5: Spectral Response Functions of the Kodak DCS-200 - Wiener Estimate.

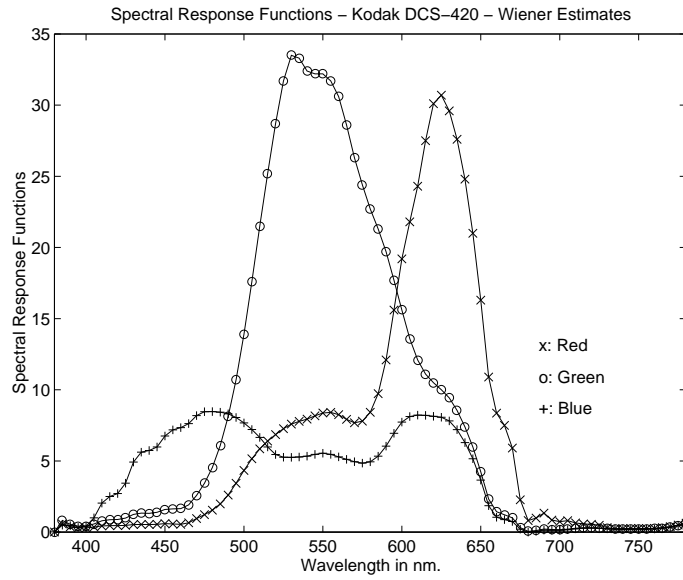


Figure 6: Spectral Response Functions of the Kodak DCS-420 - Wiener Estimate.

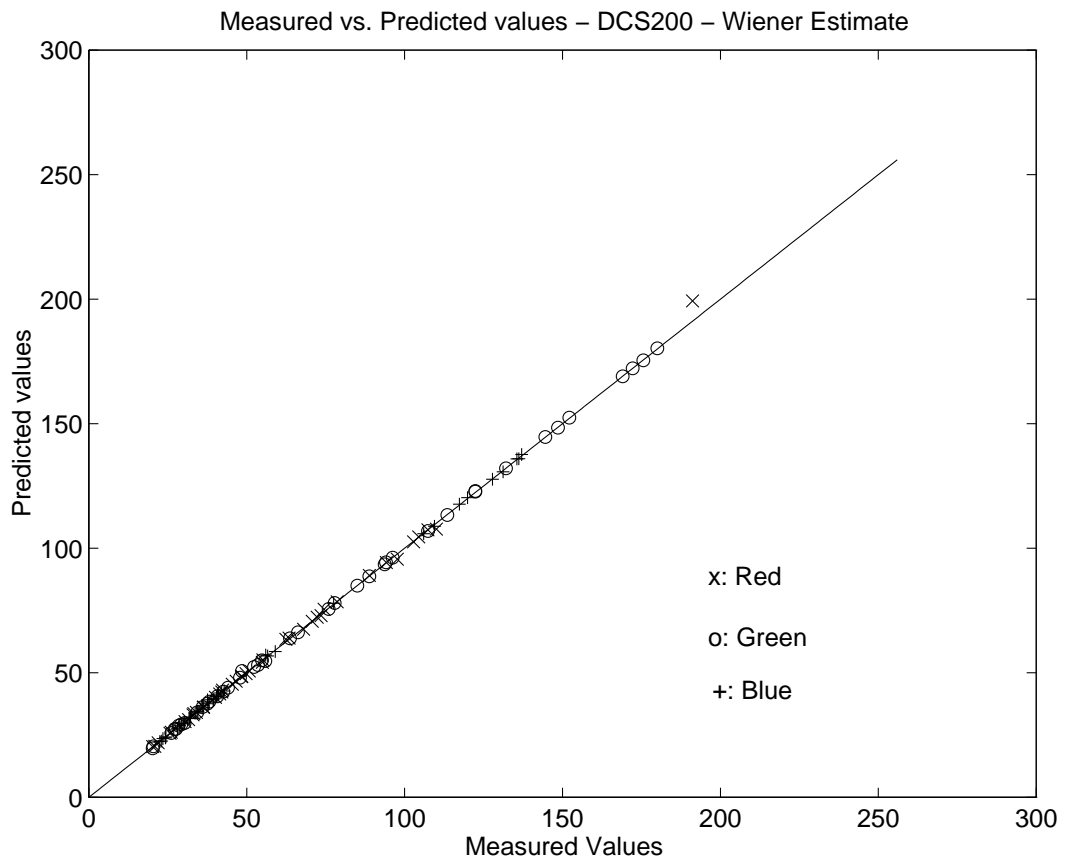


Figure 7: Measured vs. Predicted Values Kodak DCS-200 - Wiener Estimate.

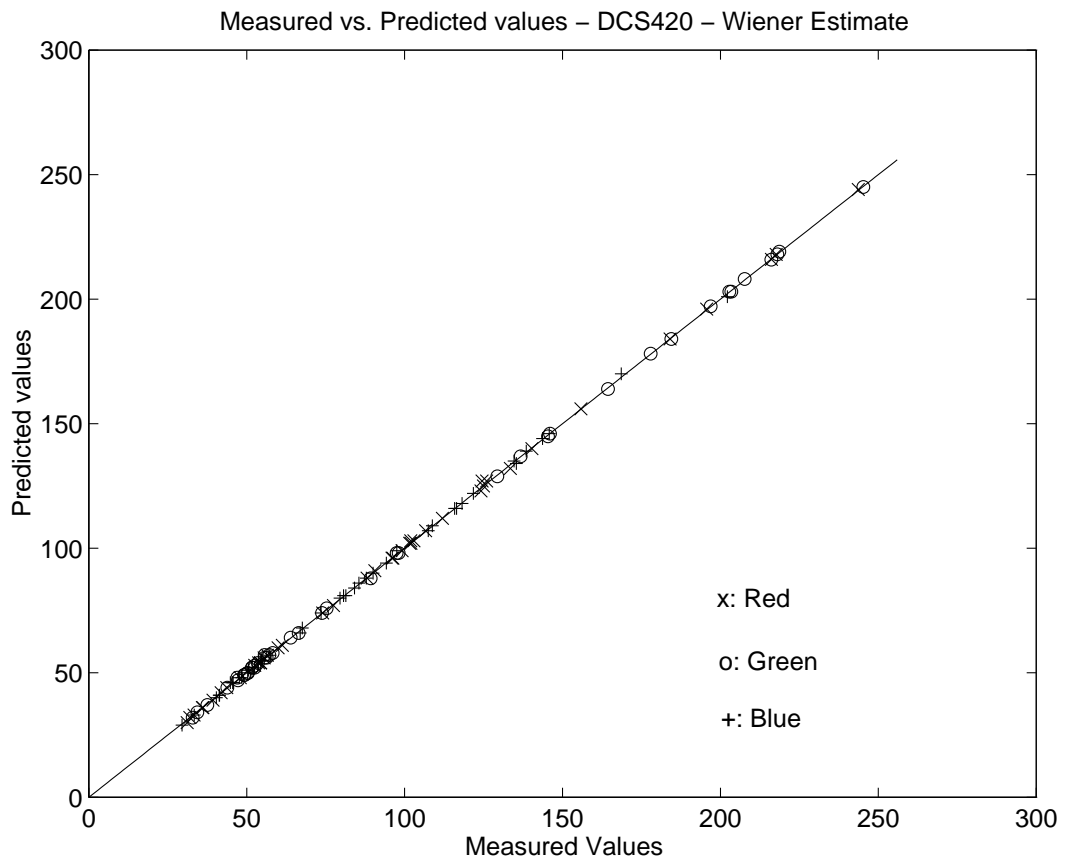


Figure 8: Measured vs. Predicted Values Kodak DCS-420 - Wiener Estimate.

The error for the Wiener estimate is very low and close to the rms value predicted by the noise statistics for both cameras. It may be compared to the far higher error in [3]. Presumably one factor driving the small error is that we used many narrowband lights to calibrate the sensors. Also, since we used narrowband lights, the simple and the Wiener estimates are very similar. This would not have been so if we had used broadband lights.

Non-linear estimation methods like Projections Onto Convex Sets (POCS) [8] are used when the Wiener estimation method gives results that clearly do not satisfy prior knowledge of the solution. For example, POCS would be used if the Wiener estimates gave unreasonable errors in the RGB values. Our Wiener estimate satisfies the three known constraints: the set of measured and predicted RGB values agree leaving room for reasonable noise, the filters are reasonably smooth, the filter transmissivities are non-negative. Hence, we did not attempt non-linear (particularly constrained) estimation methods.

5 Verification of Estimates

For the DCS-200, we tested the spectral sensitivity estimates by collecting two images of the MCC under a tungsten illuminant. For one image we used an exposure duration of $\frac{1}{30}$ second and for the other a duration of $\frac{1}{15}$ second. We compared the actual R, G, and B responses for the 24 color checker patches with values predicted from the spectral sensitivities and direct radiometric measurements of the light reaching the camera from each patch. To calculate the actual R, G, and B responses we averaged a roughly 20×20 pixel region at the center of each patch. The radiometric measurements were taken with the PhotoResearch PR-650 placed at approximately the same position as the camera. Figures 9 and 10 show the predicted vs. measured values for the simple and Wiener estimates respectively. Tables 5 and 6 list the prediction errors for the simple and Wiener estimates. The tables also list the standard deviation of the camera dark noise as well as the rms value of the variation of measured values within the 20×20 pixel region over which measurements were averaged.

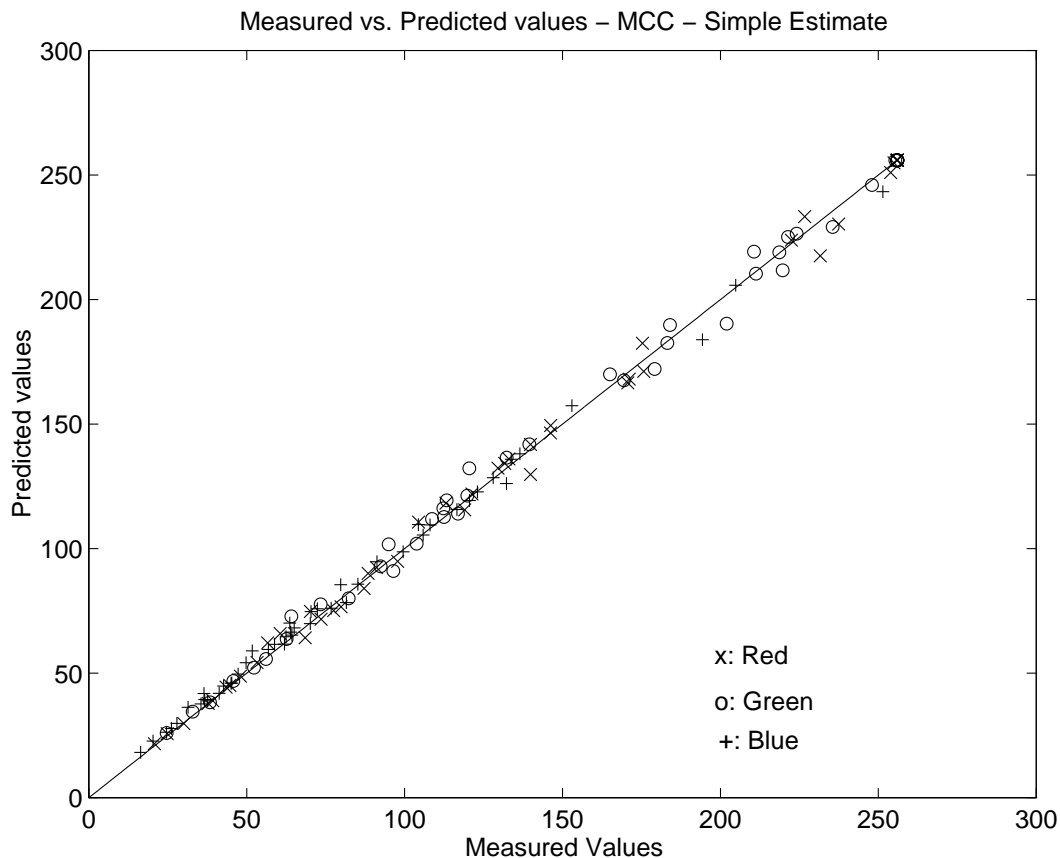


Figure 9: Measured vs. Predicted Values for MCC - Kodak DCS-200 - Simple Estimate.

Table 5: Statistics of Estimation Error for MCC - DCS-200 - Simple Estimates. RMS value of variation from linearity of DCS-200 is 1.45 [10].

| Sensor Type | Mean of Absolute Error | Mean of Absolute % Error | RMS Error | RMS of Variation in Patch | Camera Noise Std. Deviation | Maximum Absolute Error | Maximum Absolute % Error |
|-------------|------------------------|--------------------------|-----------|---------------------------|-----------------------------|------------------------|--------------------------|
| Red | 2.76 | 2.58 | 3.99 | 2.08 | 0.88 | 14.12 | 9.72 |
| Green | 2.84 | 2.40 | 4.25 | 1.96 | 0.89 | 11.78 | 13.59 |
| Blue | 2.74 | 4.55 | 3.56 | 1.83 | 0.90 | 10.44 | 15.53 |

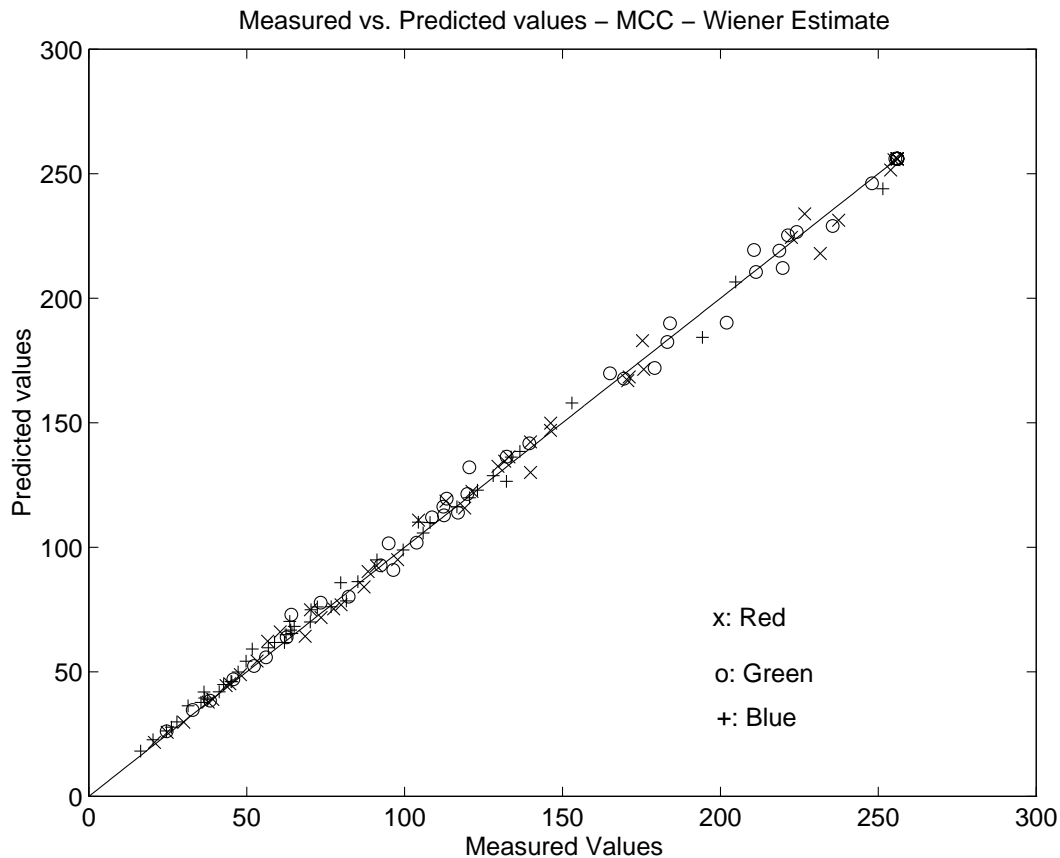


Figure 10: Measured vs. Predicted Values Kodak DCS-200 - Wiener Estimate.

Table 6: Statistics of Estimation Error for MCC - DCS-200 - Wiener Estimates. RMS value of variation from linearity of DCS-200 is 1.45 [10]

| Sensor Type | Mean of Absolute Error | Mean of Absolute % Error | RMS Error | RMS of Variation in Patch | Camera Noise Std. Deviation | Maximum Absolute Error | Maximum Absolute % Error |
|-------------|------------------------|--------------------------|-----------|---------------------------|-----------------------------|------------------------|--------------------------|
| Red | 2.80 | 2.63 | 3.97 | 2.08 | 0.88 | 13.63 | 9.97 |
| Green | 2.85 | 2.41 | 4.27 | 1.96 | 0.89 | 11.70 | 13.63 |
| Blue | 2.81 | 4.68 | 3.60 | 1.83 | 0.90 | 9.95 | 15.80 |

6 Conclusions

We have calibrated the spectral sensitivities of two digital color cameras. Both simple and Wiener estimates of these sensitivities yielded low mean square errors when they were used to predict the calibration data set. Higher but still small errors were obtained when the estimates for the DCS-200 were used to predict the average RGB values over patches in images of the MCC. The performance of the estimates is good enough for us to use them with confidence in a digital camera simulator. There is no significant difference between the two types of estimates, largely due to the fact that we used narrowband light sources for the calibration.

Appendix

Tables 7 - 9 list the set of measurements used to calibrate the DCS-200. For each sensor, the first column gives the wavelength of the monochromatic light, the second the integrated radiance of the light, the third the exposure duration, the fourth the measured response and the last the response of the camera sensor normalized by the exposure duration.

Tables 10 - 12 list the set of measurements used to calibrate the DCS-420. The columns are as in the DCS-200 measurements, in addition, the last column gives the linearized response of the camera sensor normalized by the exposure duration. Wavelengths are rounded to the nearest 5 nm increment.

Tables 13 and 14 list the simple sensor estimates and Tables 15 and 16 the Wiener sensor estimates for the DCS-200 and the DCS-420 respectively.

Table 7: Response data for DCS-200: Red sensor.

| Peak Wavelength (nm) | Radiance (0.01 watts/sr/m ²) | Exposure (sec) | Raw Response | Exposure Corrected |
|-------------------------|---|-------------------|-----------------|-----------------------|
| 440 | 1.05 | 8.0 | 20.9 | 0.911 |
| 450 | 1.27 | 8.0 | 25.7 | 1.51 |
| 455 | 1.40 | 4.0 | 20.2 | 1.66 |
| 460 | 1.49 | 4.0 | 22.0 | 2.09 |
| 470 | 1.74 | 4.0 | 26.1 | 3.12 |
| 475 | 1.93 | 4.0 | 30.5 | 4.22 |
| 480 | 1.96 | 4.0 | 34.1 | 5.12 |
| 490 | 2.22 | 4.0 | 48.4 | 8.71 |
| 500 | 2.35 | 4.0 | 70.8 | 14.3 |
| 510 | 2.48 | 2.0 | 55.1 | 20.8 |
| 520 | 2.61 | 2.0 | 68.0 | 27.2 |
| 525 | 2.73 | 1.0 | 42.4 | 28.8 |
| 530 | 2.76 | 0.5 | 31.6 | 36.0 |
| 535 | 3.00 | 0.5 | 33.3 | 39.4 |
| 540 | 3.07 | 0.5 | 36.4 | 45.5 |
| 545 | 3.35 | 0.5 | 40.1 | 53.1 |
| 550 | 3.35 | 0.5 | 41.4 | 55.7 |
| 555 | 3.69 | 0.5 | 45.4 | 63.6 |
| 560 | 3.76 | 0.5 | 46.7 | 66.2 |
| 565 | 3.97 | 0.5 | 48.4 | 69.5 |
| 570 | 4.06 | 0.5 | 49.8 | 72.4 |
| 575 | 4.27 | 0.25 | 33.0 | 77.6 |
| 580 | 4.31 | 0.25 | 36.2 | 90.5 |
| 585 | 4.49 | 0.25 | 42.1 | 114 |
| 590 | 4.48 | 0.25 | 50.8 | 149 |
| 600 | 4.60 | 0.25 | 72.3 | 235 |
| 610 | 4.80 | 0.25 | 94.2 | 323 |
| 620 | 5.00 | 0.25 | 107.4 | 375 |
| 625 | 4.90 | 0.25 | 104.5 | 363 |
| 630 | 5.09 | 0.25 | 102.8 | 357 |
| 635 | 5.00 | 0.25 | 88.8 | 301 |
| 640 | 5.19 | 0.25 | 78.6 | 260 |
| 645 | 5.11 | 0.25 | 63.4 | 199 |
| 650 | 5.26 | 0.25 | 55.0 | 165 |
| 655 | 5.39 | 0.5 | 62.4 | 97.6 |
| 670 | 5.57 | 2.0 | 110.1 | 48.2 |
| 675 | 5.60 | 8.0 | 191.2 | 22.2 |
| 685 | 5.62 | 8.0 | 97.7 | 10.5 |
| 690 | 5.64 | 8.0 | 74.5 | 7.61 |
| 705 | 5.69 | 8.0 | 73.6 | 7.49 |

Table 8: Response data for DCS-200: Green sensor.

| Peak Wavelength (nm) | Radiance (0.01 watts/sr/m ²) | Exposure (sec) | Raw Response | Exposure Corrected |
|-------------------------|---|-------------------|-----------------|-----------------------|
| 420 | 0.706 | 8.0 | 20.10 | 0.813 |
| 430 | 0.876 | 8.0 | 27.22 | 1.70 |
| 440 | 1.05 | 8.0 | 38.12 | 3.07 |
| 450 | 1.27 | 8.0 | 53.60 | 5.00 |
| 455 | 1.40 | 4.0 | 36.04 | 5.61 |
| 460 | 1.49 | 4.0 | 40.72 | 6.78 |
| 470 | 1.74 | 4.0 | 52.39 | 9.70 |
| 475 | 1.93 | 4.0 | 63.81 | 12.6 |
| 480 | 1.96 | 2.0 | 76.02 | 15.6 |
| 490 | 2.22 | 2.0 | 122.50 | 27.2 |
| 500 | 2.35 | 1.0 | 113.58 | 50.0 |
| 510 | 2.48 | 0.5 | 179.98 | 83.2 |
| 520 | 2.61 | 0.5 | 144.63 | 131 |
| 525 | 2.73 | 0.5 | 94.14 | 161 |
| 530 | 2.76 | 0.25 | 107.41 | 188 |
| 535 | 3.00 | 0.25 | 122.48 | 218 |
| 540 | 3.07 | 0.25 | 132.15 | 237 |
| 545 | 3.35 | 0.25 | 148.57 | 270 |
| 550 | 3.35 | 0.25 | 152.25 | 277 |
| 555 | 3.69 | 0.25 | 169.01 | 311 |
| 560 | 3.76 | 0.25 | 172.27 | 317 |
| 565 | 3.97 | 0.25 | 96.20 | 330 |
| 570 | 4.06 | 0.3 | 175.47 | 324 |
| 575 | 4.27 | 1.0 | 93.62 | 320 |
| 580 | 4.31 | 2.0 | 88.77 | 301 |
| 585 | 4.49 | 2.0 | 85.08 | 286 |
| 590 | 4.48 | 4.0 | 77.87 | 257 |
| 600 | 4.60 | 4.0 | 66.22 | 210 |
| 610 | 4.80 | 8.0 | 54.84 | 165 |
| 620 | 5.00 | 8.0 | 47.93 | 137 |
| 625 | 4.90 | 8.0 | 44.04 | 122 |
| 630 | 5.09 | 8.0 | 42.58 | 116 |
| 635 | 5.00 | 4.0 | 37.49 | 95.6 |
| 640 | 5.19 | 4.0 | 34.26 | 82.6 |
| 645 | 5.11 | 4.0 | 29.24 | 62.5 |
| 650 | 5.26 | 1.0 | 26.18 | 50.3 |
| 655 | 5.39 | 0.5 | 20.32 | 26.9 |
| 670 | 5.57 | 0.25 | 55.94 | 10.6 |
| 675 | 5.60 | 0.25 | 48.49 | 4.36 |
| 685 | 5.62 | 0.25 | 30.42 | 2.10 |
| 690 | 5.64 | 0.25 | 28.50 | 1.86 |
| 705 | 5.69 | 0.25 | 27.60 | 1.75 |

Table 9: Response data for DCS-200: Blue sensor.

| Peak Wavelength (nm) | Radiance (0.01 watts/sr/m ²) | Exposure (sec) | Raw Response | Exposure Corrected |
|-------------------------|---|-------------------|-----------------|-----------------------|
| 410 | 0.570 | 8.0 | 23.08 | 1.19 |
| 420 | 0.706 | 8.0 | 40.67 | 3.38 |
| 430 | 0.876 | 8.0 | 77.54 | 7.99 |
| 440 | 1.05 | 8.0 | 135.55 | 15.2 |
| 450 | 1.27 | 4.0 | 109.47 | 24.0 |
| 455 | 1.40 | 4.0 | 119.93 | 26.6 |
| 460 | 1.49 | 4.0 | 127.80 | 28.5 |
| 470 | 1.74 | 4.0 | 136.15 | 30.6 |
| 475 | 1.93 | 4.0 | 137.06 | 30.9 |
| 480 | 1.96 | 2.0 | 131.18 | 29.4 |
| 490 | 2.22 | 2.0 | 117.33 | 25.9 |
| 500 | 2.35 | 2.0 | 106.02 | 23.1 |
| 510 | 2.48 | 1.0 | 56.63 | 21.5 |
| 520 | 2.61 | 0.5 | 59.02 | 22.7 |
| 525 | 2.73 | 0.5 | 36.14 | 22.5 |
| 530 | 2.76 | 0.25 | 28.08 | 29.0 |
| 535 | 3.00 | 0.25 | 29.43 | 31.7 |
| 540 | 3.07 | 0.25 | 31.83 | 36.5 |
| 545 | 3.35 | 0.25 | 34.56 | 41.9 |
| 550 | 3.35 | 0.25 | 35.88 | 44.6 |
| 555 | 3.69 | 0.25 | 39.37 | 51.5 |
| 560 | 3.76 | 0.25 | 40.53 | 53.9 |
| 565 | 3.97 | 0.25 | 41.82 | 56.4 |
| 570 | 4.06 | 0.5 | 42.84 | 58.5 |
| 575 | 4.27 | 2.0 | 28.81 | 60.8 |
| 580 | 4.31 | 2.0 | 30.26 | 66.6 |
| 585 | 4.49 | 4.0 | 32.23 | 74.5 |
| 590 | 4.48 | 4.0 | 34.26 | 82.6 |
| 600 | 4.60 | 8.0 | 39.60 | 104 |
| 610 | 4.80 | 8.0 | 41.06 | 110 |
| 620 | 5.00 | 8.0 | 40.45 | 107 |
| 625 | 4.90 | 8.0 | 38.11 | 98.0 |
| 630 | 5.09 | 4.0 | 37.72 | 96.5 |
| 635 | 5.00 | 4.0 | 33.64 | 80.2 |
| 640 | 5.19 | 4.0 | 31.75 | 72.6 |
| 645 | 5.11 | 1.0 | 26.87 | 53.1 |
| 650 | 5.26 | 0.5 | 24.43 | 43.3 |
| 655 | 5.39 | 0.5 | 24.14 | 21.2 |
| 670 | 5.57 | 0.5 | 30.07 | 8.24 |
| 675 | 5.60 | 0.25 | 37.58 | 3.00 |
| 685 | 5.62 | 0.25 | 24.25 | 1.33 |
| 690 | 5.64 | 0.25 | 23.45 | 1.23 |
| 705 | 5.69 | 0.25 | 22.52 | 1.11 |

Table 10: Response data for DCS-420: Red Sensor.

| Peak Wavelength (nm) | Radiance (watts/sr/m ²) | Exposure (sec) | Raw Response | Linear Response | Exposure Corrected |
|-------------------------|--|-------------------|-----------------|--------------------|-----------------------|
| 385 | 0.0019 | 8 | 31.15 | 0.009 | 0.0011 |
| 390 | 0.0034 | 8 | 32.00 | 0.010 | 0.0013 |
| 405 | 0.0043 | 8 | 33.33 | 0.012 | 0.0015 |
| 410 | 0.0052 | 8 | 36.12 | 0.018 | 0.0022 |
| 425 | 0.0063 | 8 | 39.30 | 0.024 | 0.0030 |
| 430 | 0.0078 | 8 | 43.69 | 0.033 | 0.0041 |
| 445 | 0.0094 | 8 | 47.95 | 0.041 | 0.0051 |
| 450 | 0.0113 | 8 | 53.79 | 0.054 | 0.0068 |
| 465 | 0.0133 | 2 | 35.97 | 0.018 | 0.0089 |
| 470 | 0.0156 | 2 | 41.90 | 0.030 | 0.0150 |
| 480 | 0.0188 | 2 | 55.50 | 0.059 | 0.0293 |
| 490 | 0.0208 | 2 | 77.49 | 0.109 | 0.0545 |
| 500 | 0.0220 | 2 | 102.97 | 0.190 | 0.0950 |
| 510 | 0.0229 | 2 | 124.95 | 0.267 | 0.1340 |
| 520 | 0.0244 | 1 | 96.02 | 0.167 | 0.1670 |
| 530 | 0.0268 | 1 | 106.62 | 0.203 | 0.2030 |
| 540 | 0.0189 | 1 | 90.55 | 0.150 | 0.1500 |
| 550 | 0.0212 | 1 | 99.19 | 0.177 | 0.1770 |
| 560 | 0.0227 | 1 | 101.99 | 0.187 | 0.1870 |
| 570 | 0.0242 | 1 | 101.62 | 0.187 | 0.1870 |
| 580 | 0.0257 | 1 | 111.99 | 0.219 | 0.2190 |
| 590 | 0.0264 | 1 | 140.31 | 0.322 | 0.3220 |
| 600 | 0.0272 | 1 | 184.08 | 0.520 | 0.5200 |
| 610 | 0.0284 | 1 | 217.67 | 0.692 | 0.6920 |
| 620 | 0.0295 | 1 | 243.63 | 0.882 | 0.8820 |
| 630 | 0.0231 | 1 | 216.15 | 0.681 | 0.6810 |
| 640 | 0.0235 | 1 | 195.65 | 0.579 | 0.5790 |
| 650 | 0.0238 | 1 | 155.83 | 0.387 | 0.3870 |
| 655 | 0.0243 | 1 | 125.99 | 0.270 | 0.2700 |
| 670 | 0.0523 | 1 | 133.49 | 0.297 | 0.2970 |
| 675 | 0.0529 | 2 | 124.53 | 0.267 | 0.1340 |
| 690 | 0.0532 | 4 | 124.18 | 0.263 | 0.0658 |
| 695 | 0.0531 | 4 | 101.93 | 0.187 | 0.0468 |
| 705 | 0.0536 | 4 | 96.31 | 0.167 | 0.0418 |
| 710 | 0.0539 | 4 | 88.09 | 0.141 | 0.0353 |
| 725 | 0.0536 | 4 | 74.05 | 0.101 | 0.0253 |
| 730 | 0.0535 | 4 | 61.25 | 0.070 | 0.0174 |
| 745 | 0.0528 | 4 | 54.40 | 0.054 | 0.0135 |
| 750 | 0.0509 | 4 | 52.53 | 0.052 | 0.0130 |
| 760 | 0.0499 | 4 | 54.40 | 0.054 | 0.0135 |
| 770 | 0.0433 | 4 | 59.95 | 0.067 | 0.0169 |
| 780 | 0.0247 | 4 | 56.51 | 0.061 | 0.0152 |

Table 11: Response data for DCS-420: Green Sensor.

| Peak Wavelength (nm) | Radiance (watts/sr/m ²) | Exposure (sec) | Raw Response | Linear Response | Exposure Corrected |
|-------------------------|--|-------------------|-----------------|--------------------|-----------------------|
| 385 | 0.0019 | 8 | 32.87 | 0.012 | 0 |
| 390 | 0.0034 | 8 | 34.38 | 0.015 | 0 |
| 405 | 0.0043 | 8 | 37.49 | 0.02 | 0 |
| 410 | 0.0052 | 8 | 43.97 | 0.033 | 0 |
| 425 | 0.0063 | 8 | 52.41 | 0.05 | 0.01 |
| 430 | 0.0078 | 8 | 63.99 | 0.077 | 0.01 |
| 445 | 0.0094 | 8 | 75.42 | 0.104 | 0.01 |
| 450 | 0.0113 | 8 | 89.32 | 0.144 | 0.02 |
| 465 | 0.0133 | 2 | 52.50 | 0.052 | 0.03 |
| 470 | 0.0156 | 2 | 66.40 | 0.082 | 0.04 |
| 480 | 0.0188 | 2 | 97.56 | 0.173 | 0.09 |
| 490 | 0.0208 | 2 | 145.44 | 0.341 | 0.17 |
| 500 | 0.0220 | 2 | 203.37 | 0.613 | 0.31 |
| 510 | 0.0229 | 1 | 177.94 | 0.491 | 0.49 |
| 520 | 0.0244 | 1 | 218.67 | 0.698 | 0.70 |
| 530 | 0.0268 | 1 | 245.31 | 0.891 | 0.89 |
| 540 | 0.0189 | 1 | 202.76 | 0.613 | 0.61 |
| 550 | 0.0212 | 1 | 216.05 | 0.681 | 0.68 |
| 560 | 0.0227 | 1 | 218.12 | 0.692 | 0.69 |
| 570 | 0.0242 | 1 | 207.74 | 0.638 | 0.64 |
| 580 | 0.0257 | 1 | 196.87 | 0.584 | 0.58 |
| 590 | 0.0264 | 1 | 184.37 | 0.520 | 0.52 |
| 600 | 0.0272 | 1 | 164.37 | 0.424 | 0.42 |
| 610 | 0.0284 | 1 | 146.03 | 0.345 | 0.35 |
| 620 | 0.0295 | 1 | 136.76 | 0.311 | 0.31 |
| 630 | 0.0300 | 1 | 129.27 | 0.282 | 0.28 |
| 640 | 0.0235 | 1 | 98.02 | 0.173 | 0.17 |
| 650 | 0.0238 | 1 | 73.78 | 0.101 | 0.10 |
| 655 | 0.0243 | 1 | 55.66 | 0.059 | 0.06 |
| 670 | 0.0523 | 1 | 51.77 | 0.050 | 0.05 |
| 675 | 0.0529 | 2 | 47.04 | 0.038 | 0.02 |
| 690 | 0.0532 | 4 | 49.14 | 0.043 | 0.01 |
| 695 | 0.0531 | 4 | 47.17 | 0.038 | 0.01 |
| 705 | 0.0536 | 4 | 50.48 | 0.045 | 0.01 |
| 710 | 0.0539 | 4 | 56.25 | 0.059 | 0.01 |
| 725 | 0.0536 | 4 | 57.21 | 0.061 | 0.02 |
| 730 | 0.0535 | 4 | 53.68 | 0.054 | 0.01 |
| 745 | 0.0528 | 4 | 50.26 | 0.045 | 0.01 |
| 750 | 0.0509 | 4 | 49.26 | 0.043 | 0.01 |
| 760 | 0.0499 | 4 | 51.58 | 0.050 | 0.01 |
| 770 | 0.0433 | 4 | 58.16 | 0.063 | 0.02 |
| 780 | 0.0247 | 4 | 55.75 | 0.059 | 0.01 |

Table 12: Response data for DCS-420: Blue Sensor.

| Peak Wavelength (nm) | Radiance (watts/sr/m ²) | Exposure (sec) | Raw Response | Linear Response | Exposure Corrected |
|-------------------------|--|-------------------|-----------------|--------------------|-----------------------|
| 385 | 0.0019 | 8 | 29.53 | 0.0070 | 0.0009 |
| 390 | 0.0034 | 8 | 33.41 | 0.0120 | 0.0015 |
| 405 | 0.0043 | 8 | 44.82 | 0.0340 | 0.0043 |
| 410 | 0.0052 | 8 | 66.96 | 0.0840 | 0.0105 |
| 425 | 0.0063 | 8 | 97.50 | 0.1730 | 0.0216 |
| 430 | 0.0078 | 8 | 135.36 | 0.3040 | 0.0380 |
| 445 | 0.0094 | 8 | 168.59 | 0.4480 | 0.0560 |
| 450 | 0.0113 | 8 | 202.23 | 0.6090 | 0.0761 |
| 465 | 0.0133 | 2 | 107.46 | 0.2030 | 0.1020 |
| 470 | 0.0156 | 2 | 121.77 | 0.2550 | 0.1280 |
| 480 | 0.0188 | 2 | 138.51 | 0.3180 | 0.1590 |
| 490 | 0.0208 | 2 | 145.82 | 0.3450 | 0.1730 |
| 500 | 0.0220 | 2 | 143.67 | 0.3370 | 0.1690 |
| 510 | 0.0229 | 2 | 134.68 | 0.3040 | 0.1520 |
| 520 | 0.0244 | 1 | 85.54 | 0.1340 | 0.1340 |
| 530 | 0.0268 | 1 | 87.88 | 0.1410 | 0.1410 |
| 540 | 0.0189 | 1 | 73.54 | 0.1010 | 0.1010 |
| 550 | 0.0212 | 1 | 79.55 | 0.1170 | 0.1170 |
| 560 | 0.0227 | 1 | 81.39 | 0.1200 | 0.1200 |
| 570 | 0.0242 | 1 | 80.65 | 0.1200 | 0.1200 |
| 580 | 0.0257 | 1 | 84.12 | 0.1280 | 0.1280 |
| 590 | 0.0264 | 1 | 94.20 | 0.1600 | 0.1600 |
| 600 | 0.0272 | 1 | 108.79 | 0.2090 | 0.2090 |
| 610 | 0.0284 | 1 | 115.86 | 0.2330 | 0.2330 |
| 620 | 0.0295 | 1 | 118.21 | 0.2400 | 0.2400 |
| 630 | 0.0300 | 1 | 116.44 | 0.2330 | 0.2330 |
| 640 | 0.0235 | 1 | 90.00 | 0.1470 | 0.1470 |
| 650 | 0.0238 | 1 | 67.61 | 0.0870 | 0.0865 |
| 655 | 0.0243 | 1 | 50.50 | 0.0480 | 0.0475 |
| 670 | 0.0523 | 1 | 45.57 | 0.0360 | 0.0363 |
| 675 | 0.0529 | 2 | 40.39 | 0.0260 | 0.0130 |
| 690 | 0.0532 | 4 | 41.42 | 0.0280 | 0.0070 |
| 695 | 0.0531 | 4 | 41.29 | 0.0280 | 0.0070 |
| 705 | 0.0536 | 4 | 45.64 | 0.0360 | 0.0091 |
| 710 | 0.0539 | 4 | 52.49 | 0.0500 | 0.0124 |
| 725 | 0.0536 | 4 | 54.68 | 0.0560 | 0.0141 |
| 730 | 0.0535 | 4 | 51.68 | 0.0500 | 0.0124 |
| 745 | 0.0528 | 4 | 48.47 | 0.0410 | 0.0102 |
| 750 | 0.0509 | 4 | 47.64 | 0.0410 | 0.0102 |
| 760 | 0.0499 | 4 | 50.30 | 0.0450 | 0.0113 |
| 770 | 0.0433 | 4 | 57.35 | 0.0610 | 0.0152 |
| 780 | 0.0247 | 4 | 55.08 | 0.0560 | 0.0141 |

Table 13: Simple Estimates - DCS-200.

| Wavelength (nm) | Red (/watt/sr/m ² /sec) | Green (/watt/sr/m ² /sec) | Blue (/watt/sr/m ² /sec) | Wavelength (nm) | Red (/watt/sr/m ² /sec) | Green (/watt/sr/m ² /sec) | Blue (/watt/sr/m ² /sec) |
|--------------------|---------------------------------------|---|--|--------------------|---------------------------------------|---|--|
| 380 | 0 | 0 | 0 | 580 | 2100 | 6980 | 1550 |
| 385 | 0 | 0 | 0 | 585 | 2540 | 6370 | 1660 |
| 390 | 0 | 0 | 0 | 590 | 3320 | 5740 | 1840 |
| 395 | 0 | 0 | 0 | 595 | 4210 | 5150 | 2080 |
| 400 | 0 | 0 | 0 | 600 | 5100 | 4570 | 2260 |
| 405 | 0 | 0 | 0 | 605 | 5970 | 3970 | 2310 |
| 410 | 0 | 0 | 208 | 610 | 6720 | 3440 | 2290 |
| 415 | 0 | 0 | 320 | 615 | 7250 | 3050 | 2240 |
| 420 | 0 | 115 | 479 | 620 | 7500 | 2750 | 2150 |
| 425 | 0 | 155 | 679 | 625 | 7420 | 2490 | 2000 |
| 430 | 0 | 194 | 912 | 630 | 7010 | 2280 | 1890 |
| 435 | 0 | 238 | 1170 | 635 | 6020 | 1910 | 1600 |
| 440 | 86.8 | 292 | 1450 | 640 | 5020 | 1590 | 1400 |
| 445 | 121 | 356 | 1730 | 645 | 3900 | 1220 | 1040 |
| 450 | 119 | 395 | 1890 | 650 | 3150 | 957 | 825 |
| 455 | 119 | 401 | 1900 | 655 | 1810 | 499 | 394 |
| 460 | 140 | 455 | 1920 | 660 | 1120 | 255 | 169 |
| 465 | 157 | 503 | 1880 | 665 | 1000 | 214 | 150 |
| 470 | 179 | 556 | 1760 | 670 | 866 | 190 | 148 |
| 475 | 219 | 651 | 1600 | 675 | 397 | 77.9 | 53.6 |
| 480 | 261 | 796 | 1500 | 680 | 193 | 31.9 | 15.6 |
| 485 | 316 | 970 | 1340 | 685 | 187 | 37.4 | 23.7 |
| 490 | 393 | 1230 | 1170 | 690 | 135 | 33.0 | 21.8 |
| 495 | 495 | 1620 | 1060 | 695 | 53.8 | 19.5 | 10.7 |
| 500 | 607 | 2120 | 982 | 700 | 25.5 | 13.3 | 4.99 |
| 505 | 715 | 2690 | 906 | 705 | 132 | 30.8 | 19.6 |
| 510 | 837 | 3360 | 868 | 710 | 0 | 0 | 0 |
| 515 | 977 | 4150 | 889 | 715 | 0 | 0 | 0 |
| 520 | 1040 | 5020 | 869 | 720 | 0 | 0 | 0 |
| 525 | 1050 | 5910 | 827 | 725 | 0 | 0 | 0 |
| 530 | 1300 | 6800 | 1050 | 730 | 0 | 0 | 0 |
| 535 | 1310 | 7270 | 1060 | 735 | 0 | 0 | 0 |
| 540 | 1480 | 7720 | 1190 | 740 | 0 | 0 | 0 |
| 545 | 1580 | 8050 | 1250 | 745 | 0 | 0 | 0 |
| 550 | 1660 | 8270 | 1330 | 750 | 0 | 0 | 0 |
| 555 | 1720 | 8420 | 1400 | 755 | 0 | 0 | 0 |
| 560 | 1760 | 8450 | 1430 | 760 | 0 | 0 | 0 |
| 565 | 1750 | 8320 | 1420 | 765 | 0 | 0 | 0 |
| 570 | 1780 | 7970 | 1440 | 770 | 0 | 0 | 0 |
| 575 | 1820 | 7500 | 1420 | 775 | 0 | 0 | 0 |
| | | | | 780 | 0 | 0 | 0 |

Table 14: Simple Estimates - DCS-420.

| Wavelength (nm) | Red (/watt/sr/m ² /sec) | Green (/watt/sr/m ² /sec) | Blue (/watt/sr/m ² /sec) | Wavelength (nm) | Red (/watt/sr/m ² /sec) | Green (/watt/sr/m ² /sec) | Blue (/watt/sr/m ² /sec) |
|--------------------|---------------------------------------|---|--|--------------------|---------------------------------------|---|--|
| 380 | 0.00 | 0.00 | 0.00 | 580 | 8.52 | 22.7 | 4.98 |
| 385 | 0.565 | 0.807 | 0.476 | 585 | 9.86 | 21.3 | 5.38 |
| 390 | 0.368 | 0.539 | 0.445 | 590 | 12.2 | 19.7 | 6.06 |
| 395 | 0.288 | 0.410 | 0.324 | 595 | 15.6 | 17.7 | 6.92 |
| 400 | 0.293 | 0.419 | 0.408 | 600 | 19.1 | 15.6 | 7.68 |
| 405 | 0.354 | 0.566 | 0.995 | 605 | 21.8 | 13.7 | 8.08 |
| 410 | 0.427 | 0.789 | 2.03 | 610 | 24.4 | 12.1 | 8.20 |
| 415 | 0.453 | 0.870 | 2.49 | 615 | 27.5 | 11.2 | 8.20 |
| 420 | 0.453 | 0.882 | 2.70 | 620 | 29.9 | 10.5 | 8.14 |
| 425 | 0.473 | 0.988 | 3.44 | 625 | 30.5 | 10.0 | 8.04 |
| 430 | 0.527 | 1.24 | 4.90 | 630 | 29.5 | 9.40 | 7.77 |
| 435 | 0.538 | 1.33 | 5.60 | 635 | 27.5 | 8.51 | 7.16 |
| 440 | 0.526 | 1.32 | 5.73 | 640 | 24.6 | 7.36 | 6.26 |
| 445 | 0.544 | 1.39 | 5.99 | 645 | 21.0 | 5.96 | 5.12 |
| 450 | 0.598 | 1.59 | 6.74 | 650 | 16.3 | 4.24 | 3.63 |
| 455 | 0.578 | 1.65 | 7.17 | 655 | 11.1 | 2.41 | 1.95 |
| 460 | 0.556 | 1.68 | 7.35 | 660 | 8.47 | 1.48 | 1.10 |
| 465 | 0.665 | 1.95 | 7.63 | 665 | 7.37 | 1.21 | 0.871 |
| 470 | 0.958 | 2.62 | 8.17 | 670 | 5.68 | 0.950 | 0.694 |
| 475 | 1.24 | 3.47 | 8.44 | 675 | 2.52 | 0.363 | 0.246 |
| 480 | 1.56 | 4.60 | 8.46 | 680 | 1.02 | 0.0876 | 0.0319 |
| 485 | 2.00 | 6.15 | 8.42 | 685 | 1.02 | 0.116 | 0.0559 |
| 490 | 2.62 | 8.20 | 8.29 | 690 | 1.24 | 0.202 | 0.132 |
| 495 | 3.43 | 10.8 | 8.03 | 695 | 0.880 | 0.181 | 0.132 |
| 500 | 4.32 | 13.9 | 7.66 | 700 | 0.757 | 0.174 | 0.134 |
| 505 | 5.14 | 17.6 | 7.20 | 705 | 0.779 | 0.211 | 0.169 |
| 510 | 5.83 | 21.4 | 6.64 | 710 | 0.654 | 0.271 | 0.231 |
| 515 | 6.38 | 25.2 | 6.00 | 715 | 0.576 | 0.304 | 0.269 |
| 520 | 6.84 | 28.6 | 5.49 | 720 | 0.544 | 0.304 | 0.278 |
| 525 | 7.26 | 31.6 | 5.28 | 725 | 0.471 | 0.283 | 0.263 |
| 530 | 7.57 | 33.2 | 5.26 | 730 | 0.326 | 0.253 | 0.232 |
| 535 | 7.77 | 33.2 | 5.28 | 735 | 0.249 | 0.232 | 0.208 |
| 540 | 7.94 | 32.4 | 5.34 | 740 | 0.243 | 0.221 | 0.194 |
| 545 | 8.16 | 32.2 | 5.46 | 745 | 0.256 | 0.214 | 0.193 |
| 550 | 8.35 | 32.1 | 5.52 | 750 | 0.255 | 0.211 | 0.200 |
| 555 | 8.39 | 31.6 | 5.45 | 755 | 0.254 | 0.222 | 0.207 |
| 560 | 8.24 | 30.5 | 5.29 | 760 | 0.271 | 0.249 | 0.227 |
| 565 | 7.94 | 28.6 | 5.11 | 765 | 0.316 | 0.295 | 0.275 |
| 570 | 7.73 | 26.4 | 4.96 | 770 | 0.389 | 0.363 | 0.350 |
| 575 | 7.87 | 24.4 | 4.88 | 775 | 0.489 | 0.460 | 0.450 |
| | | | | 780 | 0.614 | 0.592 | 0.570 |

Table 15: Wiener Estimates - DCS-200.

| Wavelength (nm) | Red (/watt/sr/m ² /sec) | Green (/watt/sr/m ² /sec) | Blue (/watt/sr/m ² /sec) | Wavelength (nm) | Red (/watt/sr/m ² /sec) | Green (/watt/sr/m ² /sec) | Blue (/watt/sr/m ² /sec) |
|--------------------|---------------------------------------|---|--|--------------------|---------------------------------------|---|--|
| 380 | 2.33 | 2.87 | 2.95 | 580 | 2070 | 6990 | 1540 |
| 385 | 2.37 | 2.89 | 3.00 | 585 | 2500 | 6370 | 1650 |
| 390 | 2.40 | 2.91 | 3.04 | 590 | 3300 | 5730 | 1840 |
| 395 | 2.44 | 2.93 | 3.08 | 595 | 4200 | 5150 | 2080 |
| 400 | 2.48 | 2.95 | 3.13 | 600 | 5110 | 4580 | 2280 |
| 405 | 2.52 | 2.97 | 3.17 | 605 | 5990 | 3960 | 2320 |
| 410 | 2.56 | 2.99 | 211 | 610 | 6740 | 3420 | 2290 |
| 415 | 2.61 | 3.01 | 322 | 615 | 7290 | 3030 | 2250 |
| 420 | 2.65 | 118 | 480 | 620 | 7540 | 2740 | 2150 |
| 425 | 2.69 | 158 | 680 | 625 | 7470 | 2480 | 2000 |
| 430 | 2.74 | 195 | 913 | 630 | 7080 | 2290 | 1920 |
| 435 | 2.78 | 238 | 1170 | 635 | 6030 | 1910 | 1600 |
| 440 | 89.5 | 292 | 1460 | 640 | 5020 | 1600 | 1420 |
| 445 | 122 | 356 | 1730 | 645 | 3870 | 1220 | 1020 |
| 450 | 120 | 395 | 1900 | 650 | 3200 | 975 | 850 |
| 455 | 118 | 399 | 1910 | 655 | 1740 | 475 | 368 |
| 460 | 139 | 453 | 1920 | 660 | 1070 | 226 | 149 |
| 465 | 156 | 499 | 1880 | 665 | 1010 | 213 | 150 |
| 470 | 178 | 551 | 1760 | 670 | 904 | 200 | 160 |
| 475 | 218 | 645 | 1600 | 675 | 367 | 70.7 | 46.3 |
| 480 | 259 | 788 | 1500 | 680 | 174 | 26.9 | 10.6 |
| 485 | 313 | 959 | 1340 | 685 | 192 | 38.5 | 25.1 |
| 490 | 390 | 1210 | 1160 | 690 | 140 | 34.5 | 23.2 |
| 495 | 494 | 1610 | 1050 | 695 | 67.0 | 22.5 | 13.0 |
| 500 | 606 | 2110 | 979 | 700 | 49.1 | 18.3 | 8.61 |
| 505 | 714 | 2680 | 902 | 705 | 164 | 37.3 | 24.3 |
| 510 | 836 | 3340 | 861 | 710 | 33.4 | 6.81 | 4.85 |
| 515 | 976 | 4140 | 884 | 715 | 32.9 | 6.77 | 4.78 |
| 520 | 1040 | 5010 | 863 | 720 | 32.4 | 6.72 | 4.71 |
| 525 | 1040 | 5920 | 810 | 725 | 31.9 | 6.67 | 4.64 |
| 530 | 1310 | 6830 | 1060 | 730 | 31.4 | 6.63 | 4.58 |
| 535 | 1310 | 7280 | 1050 | 735 | 30.9 | 6.58 | 4.51 |
| 540 | 1480 | 7730 | 1190 | 740 | 30.4 | 6.53 | 4.45 |
| 545 | 1580 | 8060 | 1250 | 745 | 29.9 | 6.49 | 4.38 |
| 550 | 1660 | 8280 | 1330 | 750 | 29.4 | 6.44 | 4.32 |
| 555 | 1730 | 8440 | 1400 | 755 | 28.9 | 6.40 | 4.26 |
| 560 | 1760 | 8470 | 1440 | 760 | 28.5 | 6.35 | 4.20 |
| 565 | 1750 | 8350 | 1420 | 765 | 28.0 | 6.31 | 4.14 |
| 570 | 1780 | 7990 | 1440 | 770 | 27.6 | 6.27 | 4.08 |
| 575 | 1790 | 7510 | 1410 | 775 | 27.1 | 6.22 | 4.02 |
| | | | | 780 | 26.7 | 6.18 | 3.96 |

Table 16: Wiener Estimates - DCS-420.

| Wavelength (nm) | Red (/watt/sr/m2/sec) | Green | Blue | Wavelength (nm) | Red (/watt/sr/m2/sec) | Green | Blue |
|--------------------|--------------------------|--------|--------|--------------------|--------------------------|--------|---------|
| 380 | 0.00697 | 0.0104 | 0.0134 | 580 | 8.42 | 22.7 | 4.94 |
| 385 | 0.572 | 0.817 | 0.489 | 585 | 9.73 | 21.3 | 5.34 |
| 390 | 0.373 | 0.547 | 0.456 | 590 | 12.1 | 19.7 | 6.04 |
| 395 | 0.292 | 0.417 | 0.333 | 595 | 15.6 | 17.7 | 6.94 |
| 400 | 0.297 | 0.424 | 0.416 | 600 | 19.2 | 15.6 | 7.73 |
| 405 | 0.357 | 0.571 | 1.00 | 605 | 21.8 | 13.6 | 8.12 |
| 410 | 0.430 | 0.794 | 2.04 | 610 | 24.3 | 12.1 | 8.22 |
| 415 | 0.455 | 0.874 | 2.50 | 615 | 27.5 | 11.1 | 8.20 |
| 420 | 0.455 | 0.884 | 2.71 | 620 | 30.1 | 10.5 | 8.14 |
| 425 | 0.474 | 0.989 | 3.44 | 625 | 30.7 | 10.0 | 8.07 |
| 430 | 0.529 | 1.24 | 4.92 | 630 | 29.6 | 9.43 | 7.81 |
| 435 | 0.539 | 1.33 | 5.62 | 635 | 27.6 | 8.55 | 7.20 |
| 440 | 0.527 | 1.32 | 5.73 | 640 | 24.8 | 7.39 | 6.29 |
| 445 | 0.544 | 1.39 | 5.98 | 645 | 21.0 | 5.98 | 5.15 |
| 450 | 0.600 | 1.59 | 6.75 | 650 | 16.3 | 4.23 | 3.65 |
| 455 | 0.574 | 1.63 | 7.18 | 655 | 10.9 | 2.32 | 1.86 |
| 460 | 0.546 | 1.65 | 7.34 | 660 | 8.36 | 1.43 | 1.04 |
| 465 | 0.652 | 1.91 | 7.62 | 665 | 7.50 | 1.22 | 0.879 |
| 470 | 0.951 | 2.58 | 8.19 | 670 | 5.91 | 1.00 | 0.742 |
| 475 | 1.23 | 3.43 | 8.46 | 675 | 2.27 | 0.317 | 0.206 |
| 480 | 1.54 | 4.54 | 8.47 | 680 | 0.816 | 0.0490 | -0.0001 |
| 485 | 1.98 | 6.09 | 8.43 | 685 | 0.989 | 0.109 | 0.05 |
| 490 | 2.60 | 8.12 | 8.31 | 690 | 1.33 | 0.219 | 0.145 |
| 495 | 3.43 | 10.7 | 8.05 | 695 | 0.843 | 0.179 | 0.132 |
| 500 | 4.33 | 13.9 | 7.67 | 700 | 0.740 | 0.168 | 0.129 |
| 505 | 5.15 | 17.6 | 7.21 | 705 | 0.803 | 0.208 | 0.165 |
| 510 | 5.85 | 21.5 | 6.65 | 710 | 0.646 | 0.275 | 0.234 |
| 515 | 6.40 | 25.2 | 5.98 | 715 | 0.571 | 0.308 | 0.274 |
| 520 | 6.85 | 28.7 | 5.45 | 720 | 0.550 | 0.307 | 0.282 |
| 525 | 7.27 | 31.7 | 5.26 | 725 | 0.482 | 0.284 | 0.265 |
| 530 | 7.59 | 33.5 | 5.25 | 730 | 0.315 | 0.251 | 0.231 |
| 535 | 7.78 | 33.3 | 5.28 | 735 | 0.240 | 0.231 | 0.206 |
| 540 | 7.94 | 32.4 | 5.34 | 740 | 0.240 | 0.220 | 0.193 |
| 545 | 8.17 | 32.2 | 5.46 | 745 | 0.259 | 0.214 | 0.191 |
| 550 | 8.37 | 32.2 | 5.54 | 750 | 0.255 | 0.209 | 0.200 |
| 555 | 8.41 | 31.7 | 5.46 | 755 | 0.252 | 0.219 | 0.205 |
| 560 | 8.25 | 30.6 | 5.29 | 760 | 0.267 | 0.246 | 0.223 |
| 565 | 7.92 | 28.6 | 5.11 | 765 | 0.311 | 0.290 | 0.270 |
| 570 | 7.68 | 26.3 | 4.95 | 770 | 0.385 | 0.359 | 0.346 |
| 575 | 7.80 | 24.4 | 4.85 | 775 | 0.497 | 0.468 | 0.458 |
| | | | | 780 | 0.633 | 0.611 | 0.589 |

References

- [1] Brainard, D. H., "Bayesian method for Reconstructing Color Images from Trichromatic Samples", IS&T, 47th Annual Conference, pp. 375-380, 1994.
- [2] Horn, B. K. P., "Exact reproduction of colored images", Computer Vision, Graphics and Image Processing vol. 26, pp. 135-167, 1984.
- [3] Hubel, P. M., Sherman, D. and Farrell, J. E., "A Comparison of Methods of Sensor Spectral Sensitivity Estimation", Proc., IS&T/SID 2nd. Color Imaging Conference: Color Science, Systems and Applications, pp. 45:48, 1994.
- [4] Freeman, W. T. and Brainard, D. H., "Bayesian decision theory, the maximum local mass estimate, and color constancy", Proceedings of the 5th International Conference on Computer Vision, pp. 210-217, 1995.
- [5] Maloney, L. T. and Wandell, B. A., "Color constancy: a method for recovering surface spectral reflectances", Journal of the Optical Society of America-A vol. 3, pp. 29-33, 1986.
- [6] Pratt, W. K., *Digital Image Processing*, John Wiley & Sons: New York, 1978.
- [7] Sharma, G. and Trussell, H. J., "Figures of merit for color scanners and cameras", in review, IEEE Trans. Image Proc.
- [8] Trussell, H. J., and Civanlar, M. R., "The Feasible Solution in Signal Restoration", IEEE Transactions on Acoustics, Speech, and Signal Processing, Vol ASSP-32, pp 201-212, 1984.
- [9] Vora, P. L., Harville, M. L., Farrell, J. E., Tietz, J. D., Brainard, D. H., "Digital image capture: synthesis of sensor responses from multispectral images", to be presented at the IS&T/SPIE Symposium on Electronic Imaging: Science and Technology, Feb. 1997.

- [10] Vora, P. L., Farrell, J. E., Tietz, J. D., Brainard, D. H., "Digital color cameras - 1 - Response models", Hewlett-Packard Company Technical Report, March 1997.
- [11] Vora, P. L., Harville, M. L., Farrell, J. E., Tietz, J. D., Brainard, D. H., "Digital camera simulation: synthesis of sensor responses from multispectral images", Hewlett-Packard Company Technical Report, in preparation.
- [12] Vora, P. L., and Trussell, H. J., "Measure of Goodness of a Set of Colour Scanning Filters", Journal of the Optical Society of America - A, Vol. 10, No. 7, July 1993.
- [13] Vrhel, M. J., and Trussell, H. J., "Filter Considerations in Color Correction", IEEE Transactions on Image Processing, Vol. 3, No. 2, pp. 147-161, Mar. 1994.
- [14] Wandell, B. A., "Color rendering of camera data", Color Research and Application, Supplement 11, S30-S33, 1986.
- [15] Wolski, M., Allebach, J. P., Bouman, C. A. and Walowit, E., "Optimization of sensor response functions for colorimetry of reflective and emissive objects", IEEE Trans. Image Proc., vol. 5, no. 3, pp. 507-517, Mar. 1996.
- [16] *Programmer's Reference Manual Models: DCS-200ci, DCS-200mi, DCS-200c, DCS-200m.* Eastman Kodak Company, December 1992.
- [17] *MATLAB High-Performance Numeric Computation and Visualization Software, Reference Guide,* The MathWorks, Inc., 1992.

List of Tables

| | | |
|----|--|----|
| 1 | Statistics of Estimation Error - DCS-200 - Simple Estimate. | 5 |
| 2 | Statistics of Estimation Error - DCS-420 - Simple Estimate. | 5 |
| 3 | Statistics of Estimation Error - DCS-200 - Wiener Estimates. | 10 |
| 4 | Statistics of Estimation Error - DCS-420 - Wiener Estimates. | 10 |
| 5 | Statistics of Estimation Error for MCC - DCS-200 - Simple Estimates. . . . | 15 |
| 6 | Statistics of Estimation Error for MCC - DCS-200 - Wiener Estimates. . . . | 16 |
| 7 | Response data for DCS-200: Red sensor. | 18 |
| 8 | Response data for DCS-200: Green sensor. | 19 |
| 9 | Response data for DCS-200: Blue sensor. | 20 |
| 10 | Response data for DCS-420: Red Sensor. | 21 |
| 11 | Response data for DCS-420: Green Sensor. | 22 |
| 12 | Response data for DCS-420: Blue Sensor. | 23 |
| 13 | Simple Estimates - DCS-200. | 24 |
| 14 | Simple Estimates - DCS-420. | 25 |
| 15 | Wiener Estimates - DCS-200. | 26 |
| 16 | Wiener Estimates - DCS-420. | 27 |

List of Figures

| | | |
|----|--|----|
| 1 | Spectral Response Functions - Kodak DCS-200 - Simple Estimate. | 6 |
| 2 | Spectral Response Functions - Kodak DCS-420 - Simple Estimate. | 6 |
| 3 | Measured vs. Predicted Values - Kodak DCS-200 - Simple Estimate. | 7 |
| 4 | Measured vs. Predicted Values - Kodak DCS-420 - Simple Estimate. | 8 |
| 5 | Spectral Response Functions - Kodak DCS-200 - Wiener Estimate. | 11 |
| 6 | Spectral Response Functions - Kodak DCS-420 - Wiener Estimate. | 11 |
| 7 | Measured vs. Predicted Values - Kodak DCS-200 - Wiener Estimate. | 12 |
| 8 | Measured vs. Predicted Values - Kodak DCS-420 - Wiener Estimate. | 13 |
| 9 | Measured vs. Predicted Values for MCC - Kodak DCS-200 - Simple Estimate. | 15 |
| 10 | Measured vs. Predicted Values for MCC - Kodak DCS-200 - Wiener Estimate. | 16 |